International Journal of ChemTech Research
CODEN (USA): IJCRGG ISSN: 0974-4290
Vol.7, No.3, pp 1578-1585, 2014-2015

ICONN 2015 [4th - 6th Feb 2015]
International Conference on Nanoscience and Nanotechnology-2015
SRM University, Chennai, India

Ullmann Condensation Via O-Arylation of Phenol using Nano Copper Derived From Copper(II) Precursor

Arunachalam Dinesh Karthik[1] and Kannappan Geetha[2]*

[1]Department of Chemistry, K. M. G. College of Arts and Science, Gudiyattam, 635 803 Vellore.Dt. Tamil Nadu, India
[2*] Department of Chemistry, Muthurangam Govt. Arts College(Autonomous), Vellore - 632 002, Tamil Nadu, India

Abstract: Copper nanoparticles provide an efficient, economic, and novel method for the synthesis of diaryl ethers via Ullmann condentation. This method provides a wide range of substrate applicability and avoids the use of a heavy metal co-catalyst and gives diaryl ethers in satisfactory yields. The action of nanoparticles copper catalysts using thermal decomposition method with a mean particle size of 75 nm in the Ullmann ether synthesis is reported.
Keywords: Metallic nanoparticles, Copper, thermal reduction Inorganic precursor, X-ray diffraction and Ullmann.

Introduction

Copper and the compounds of Au, Ag, Pd and Pt are widely used these days. Copper has an excellent electrical conductivity. Due to relatively low costs, this metal plays a significant role in modern electronic circuit[1]. Because of its excellent electrical conductivity, catalytic behaviour, good compatibility and surface enhanced Raman scattering activity, Copper nanoparticles have drawn the attention of scientists to be used as essential component in the future nano devices[2]. Copper nanowires are used in nanoelectronics and have application possibilities for magnetic devices, nano sensors, electron emitters and other electronic applications[3]. Copper nanoparticles have been explored to be used as nanoprobes in medicines and bio-analytical areas[4] High temperature superconductivity materials are mostly prepared from CuO based compounds[5]. Similarly semiconducting anti ferromagnetic materials are also synthesized from Copper nanoparticles are a class of materials with properties which differ from their characteristics and find use in different areas such as electronic, magnetic, pharmaceutical, cosmetic energy, catalytic and materials applications. A large number of nanoparticles have been prepared most frequently by dispersion of performed polymers[5]. Solvent evaporation method and ionic gelation method. In order to produce small particle size, often a high speed homogenization or ultrasonication may be employed. Conventional methods such as solvent extraction evaporation, includes $NaBH_4$[6], Cu, Ni, Co complexes[7] and macrocyclic ligands[8]. This method avoids the use of hazardous polymers and solvents which are required in excess amounts. The most popular Cu(I)[9] and Cu(0)[10] nanoparticles emerged as useful and unique green catalysts whose efficiency is attributed to their characteristic high surface to volume ratio that translates into more number of active sites per unit area compared to dominate the properties of matter

as size is reduced to nanoscale[11]. A large number of nanoparticles have been prepared most frequently by dispersion of performed polymers solvent evaporation method and ionic gelation method[12]. In order to produce small particle size, often a high speed homogenization or ultrasonication may be employed[13]. Conventional methods such as solvent extraction evaporation[14], solvent diffusion and organic phase separation methods are hazardous to the environment as well as physiological system. The most popular Cu(I) and Cu(0) nanoparticles emerged as useful and unique green catalysts[15].

Experimental

All the chemicals and reagents used were of analytical grade and were used as received without further purification, and a series of experiments were processed in order to synthesize by employing different method.

Synthesis of the Copper nanoparticles

Copper(II) succinate precursor was prepared by adding drop wise the solution of disodium succinate to copper sulphate solution in the ratio of 2:1 under magnetic stirring for 15 minutes. The resulting green precipitate was centrifuged and washed with ethanol several times. The product was dried. The Copper(II) succinate was characterized by FT IR[16]. In this synthesis, nanoparticles were prepared by the thermal reduction of the Copper(II) succinate – oleylamine complex as a precursor[17-21].

O-Arylation of Phenol Using Nano Copper *(Cu np)*

To explore catalytic methodology[22] and the role of transition metal nanoparticle in organic trans formations, is reported here in recyclable Copper nanoparticles as the catalyst for an efficient synthesis of diphenyl ethers. Initially to examine the catalytic activity of Copper nanoparticles, the reaction mixture of phenol (1.0 mmol) with bromobenzene (1.0 mmol) in the presence of (0.02 mmol) of Copper nanoparticles (Cu np) and KOH (2.0 equiv) as base in DMSO (5 mL) was heated at 50–60°C for 4 hrs in ultrasonication bath. (Scheme1). The diaryl ether was formed in 91% yield in 4 h. The progress of the reaction was monitored by TLC. After cooling the reaction mixture at room temperature, the precipitated catalyst was separated by simple filtration and filtrate so obtained was diluted with ethyl acetate (10 ml)[23]. The solvent was evaporated under vacuum to give the crude product to yield the expected product as yellowish oil. The products were analyzed by FT IR, ^{1}H &^{13}C NMR analysis. FTIR: (C=C) - Aromatic ring 1597 cm^{-1}, (C-O) Aromatic ethers 1028 cm^{-1} **Figure 2 (b).** ^{1}H NMR ($CDCl_3$): Aromatic Protons (δ ppm) (7.13-7.15) ^{13}C NMR (δ ppm) (115.6-128.6) **Figure 8**.

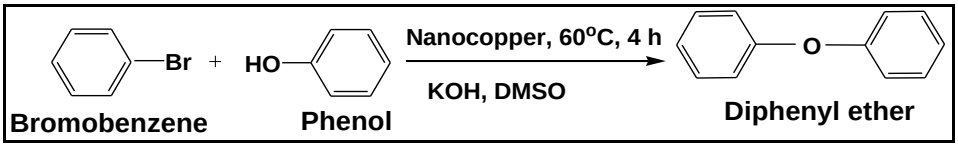

Scheme 1. Nanocopper catalyzed reaction of bromobenzene with phenol.

Results and discussion

UV Visible Spectra

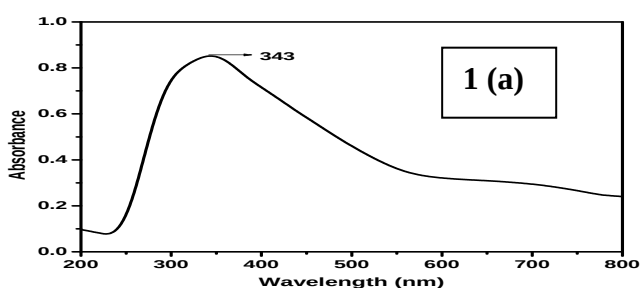

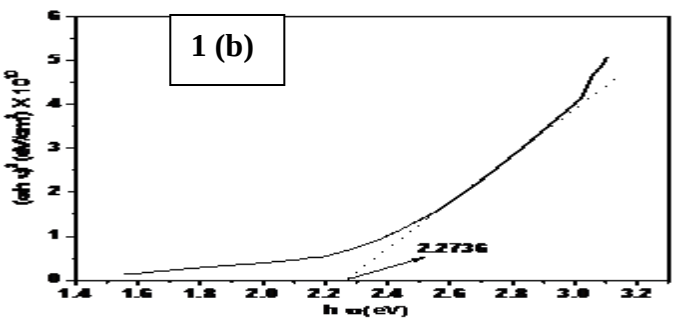

Figure 1. (a) The UV Visible absorption spectrum of the Copper nanoparticles coated by oleylamine.
Figure 1. (b) Tauc plot of UV Visible absorption data of as synthesized Copper nanoparticles for the calculation of bandgap energy.

The UV– visible spectra of Copper and its oxide nanoparticles are shown in Figure 1. Because of the surface Plasmon resonance effect, a Copper and its oxide nanoparticles usually exhibit absorption bands in the range of 300- 400nm. This kind of stabilization of Copper and its oxide nanoparticles was due to the capping of particles by oleylamine in thermal process. The optical band gap of the as by synthesized nanoparticles is calculated using the Tauc relation $\alpha h\upsilon = (h\upsilon - Eg)^n$, where $h\nu$ is the incident photon energy and n is the exponent that determines the type of electronic transition causing the absorption and can take the values 1/2, 2/3, 2 and 3/2. The best linear relationship is obtained by plotting $(\alpha h\upsilon)^2$ against $h\upsilon$, indicating that the optical band gap of these nanoparticles is due to a direct allowed transition[24]. Tauc plot for as synthesized nanoparticles is shown in figure 1 (b). The band gap of as synthesized Copper and its oxide nanoparticles is determined from the intercept of the straight line at $\alpha = 0$, which is found to be 2.2736 eV[26]

IR measurement

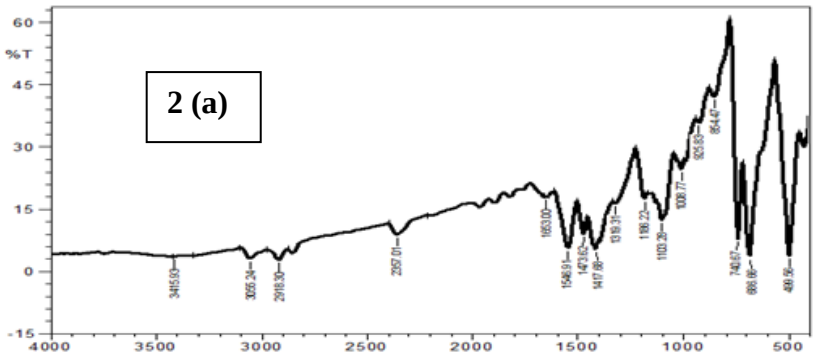

Figure 2 (a). F T IR spectra of Copper nanoparticles coated by oleylamine.

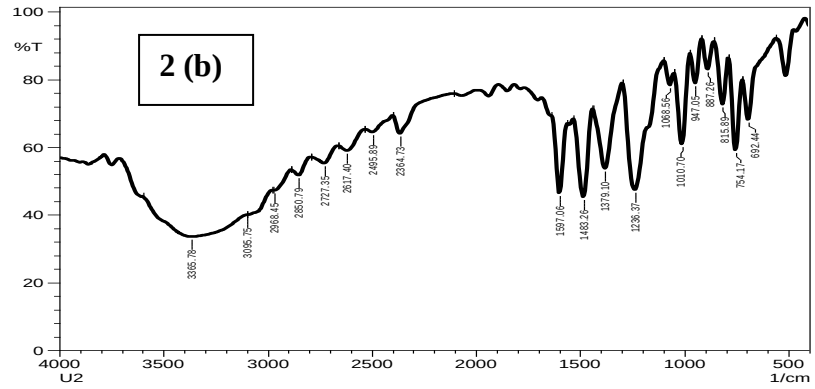

Figure 2 (b). F T IR spectra of diphenyl ethers using Copper nanoparticles is a catalyst.

Figure 2(a) Shows FT IR Spectrum of Copper nanoparticles with oleylamine as capping agent in the region of 4000cm^{-1} – 400cm^{-1}. FT IR helped in ascertaining the functional group of Copper(II) succinate precursor and the formation of nanoparticles. The organic molecules are a part of the nanoparticles is clear from the spectra. As shown in **Figure 2(a)**, peaks corresponding to P–Ph stretching at 780 cm^{-1}, rocking and bending mode of the methylene group **ω** (CH_2) at 1184cm^{-1}, benzene ring at 686 cm^{-1} can be seen clearly.

The only difference among these characteristic peaks is either change in the peak intensity or a slight shift in the peak position. For example, the peak position of the longitudinal modes of free oleylamine and free TPP shifts to lower wave numbers after TPP and oleylamine are adsorbed on the surface of the nanoparticles. The FT-IR of the copper nanoparticles shows the intense adsorption peaks at 2926cm^{-1} attributed to the alkyl chains of oleylamine. This indicates that oleylamine is bound on the surface through the unpaired electron couple of the amine group. So the oleylamine and TPP serves as the capping ligand that controls growth. Triphenylphosphine (TPP) was widely used in the synthesis of phosphine stabilized cobalt or other metal nanoparticles [27].

XRD Measurement

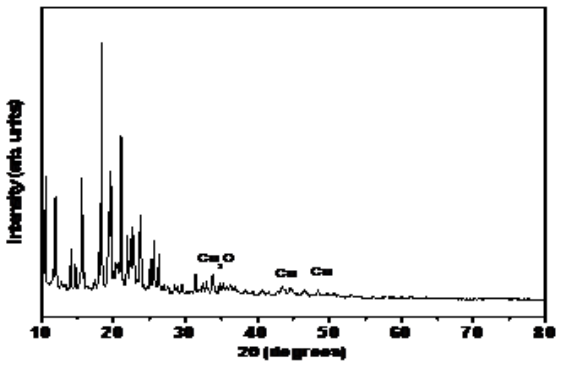

Figure 3. XRD pattern of the Copper and Copper oxide nanoparticles.

Figure 3. Shown in X-ray powder diffraction (XRD) pattern of nanoparticles at room temperature. X – Ray diffraction is one of the most important characterization tool used in nanomaterial's research field. The copper nanoparticles Synthesized got oxidized in due course. The XRD pattern is consistent with the Spectrum of Cu and CuO nanoparticles. Bragg's reflections for nanoparticles was observed in XRD pattern at 2θ value 38.48, 43.73, 51.39 and 73.42 representing Cu [110], [111], [200] and [220] and Cu [110], [211], [311] planes of FCC structure of copper with the space group of F_{m3m} (JCPDS No. 4–0836). Powder X-ray Analysis Data analysis shows the nanoparticles system is hexagonal lattice, Type P, the Lattice parameter was a= 4.9168 b= 4.9168 c= 5.408 and Alpha= 90 Beta= 90 Gama=120 Radiation, Cu Wavelength: 1.5418 Å. The size of the nanoparticles estimated from Debye - Scherer equation is about average 75 nm [28].

Peak Indexing

Indexing is the process of determining the unit cell dimensions from the peak positions. It is the first step in diffraction pattern analysis. To index a powder diffraction pattern it is necessary to assign Miller Indices (hkl) to each peak.

XRD analysis of the prepared sample of nanoparticles was done by a Goniometer (Ultima3 theta-theta gonio, under 40kV/30mA - X-Ray, 2θ / θ – Scanning mode, Fixed Monochromator). Data was taken for the 2θ range of 10 to 80 degrees with a step of 0.02 degree. Indexing process of powder diffraction pattern was done and Miller Indices (hkl) to each peak was assigned in first step[28].

Table 1. Simple peak indexing

Peak position, 2θ	**1000xSin^2 θ**	**1000xSin^2 θ/46**	**1000xSin^2 θ/46 (Std value)**	**Reflection**	**Remarks**
43.54	138	3	3	(1 1 1)	$1^2+1^2+1^2= 3$
50.69	184	4	4	(2 0 0)	$2^2+0^2+0^2=4$
74.35	328	7.13	8	(2 2 0)	$2^2+2^2+0^2= 8$

Indexing has been done in two different methods and data are in Table.1 & Table.2. Both these methods bring the same result. In table.1, it is needed to find a dividing constant. The values in the 3rd column become integers (approximately). Here, the constant is 46 (= 184−138). Moreover, the high intense peak for ***fcc*** materials is generally (111) reflection, which is observed in the sample.

Table 2. Peak indexing from d – spacing

2θ	**D**	**1000/d^2**	**(1000/d^2) / 77.32**	**hkl**
43.54	1.8588	232.07	3.01	111
50.69	1.8009	310.02	4.01	200
74.35	1.2760	616.11	8.00	220

Three peaks at 2θ values of 43.54, 50.69, and 74.35 deg corresponding to (111), (200), and (220) planes of copper were observed and compared with the standard powder diffraction card of JCPDS, copper file No. 04–0836. Table.3 shows the experimentally obtained X-ray diffraction angle and the standard diffraction angle of Cu specimen. The XRD study confirms / indicates that the resultant particles are ***(fcc)*** Copper nanoparticles[28,29].

Table 3. Peak indexing from d – spacing

2θ of the intense peak (deg)	θ of the intensepeak (deg)	FWHM of Intense peak (β) radians	Size of the particle (D) nm	d spacing nm	Plane	Material	Microstrain
43.54	21.77	0.1181	73.0	1.8588	(111)	Cu	0.07392
50.69	25.35	0.1181	75.0	1.8009	(200)	Cu	0.06231
74.35	37.18	0.1378	72.8	1.2760	(220)	Cu	0.04542

Particle Size Calculation

The existence of sharp peaks indicates that the synthesized nanoparticles are polycrystalline in nature [27]. One can calculate the values of average crystallite size Debye - Scherer formula (*D*) from eq (1), d-Spacing the value of d (the inter planar spacing between the atoms) is calculated from eq (2) and microstrain (ε) from eq (3) formation XRD spectrum using the following equations:

$[D = 0.9\,\lambda / \beta\cos\theta]$. …….. (1)

Bragg's Law: $2d\sin\theta = n\,\lambda$ …….. (2)

$$d = \frac{\lambda}{2\sin\theta} \quad (n=1)$$

Wavelength λ = 1.5418 Å for Cu Ka

$\varepsilon = \beta / 4\tan\theta$ …… (3)

The calculated d-spacing and micro strain details are in **Table 3**.

TGA & DTA analysis

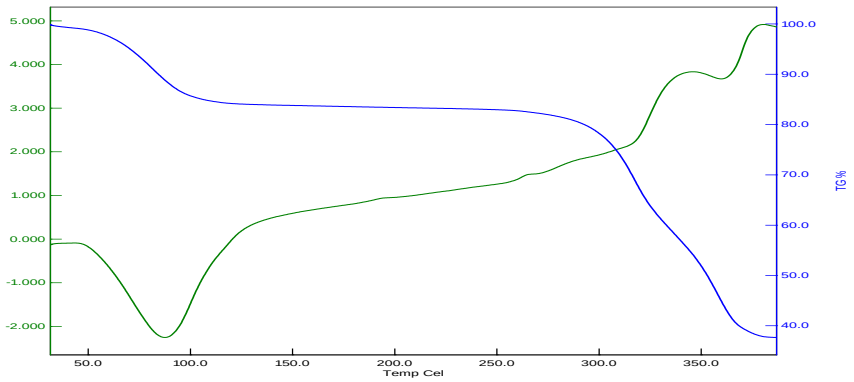

Figure 4. TGA and DTA of Copper(II) succinate.

The TGA & DTA curve of the as prepared precursor is shown in **Figure 4**. To examine the thermal stability of the bulk powder compound Copper(II) succinate, thermal gravimetric (TGA) and Differential thermal analysis (DTA) were carried out between 10 to 400° C under nitrogen flow (Figure 4). The compound is stable up to 240° C. Decomposition of compound occurs between 268° C to 296° C with the mass loss of 59%. The DTA curves display two endothermic peak effect at 180° C and 275° C for the powder of Compound.

Cyclic Voltagramm (CV)

Figure 5 show the Cyclic Voltagramm (CV) of the copper nanoparticles was recorded in DMF with 0.1 M tetrabutylammonium perchlorate as supporting electrolyte in the potential range -2 to + 0.1 V, with a conventional three electrode system composed of a platinum auxiliary, Glassy carbon working electrode and

Calomel (Saturated KCl) reference electrode. The reductive peaks correspond to Cu (II)/Cu (I) and Cu (0). i.e CuO → Cu_2O →Cu. The redox peak currents increase linearly with increase in the scan rate from 20 to 100 Mvs^{-1} **(Figure 5)** the oxidative peak corresponds to Cu → Cu_2O →CuO.

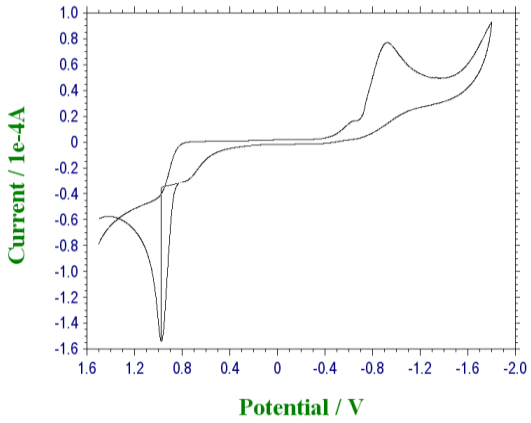

Figure 5. C V spectrum of the Copper oleylamine caped nanoparticles.

SEM and AFM

The morphology of the product was examined by SEM. **Figure 6** Depicts the SEM pictures of a sample of nanoparticles. From the micrograph, it was observed that the nanoparticles are agglomerated. When the reaction was carried out at 245°C, most organic molecules decomposed and since only a few oleylamine molecules were adsorbed on the nanoparticles, a loose solid rod-like morphology was finally produced. This observation alludes to the size effect of the nanoparticles. This kind of stabilization of nanoparticles is due to the capping of particles by oleylamine on thermal treatment.

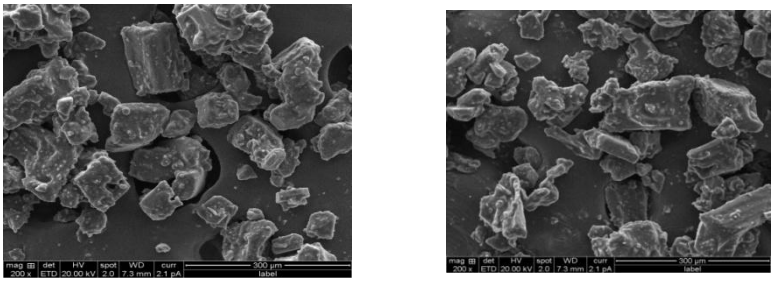

Figure 6. (a) SEM images of the Agglomerated Copper nanoparticles.

Figure 7 shows the topographical image of oleylamine modified nanoparticles[AFM] (transfer pressure is 20 mN/m, mica substrate) acquired simultaneously at the same sample location. results showed that the modified Copper and Copper oxide nanoparticle has typical core shell structure. The oleylamine capped copper nanoparticle was composed of many nanoparticles arranged closely and orderly. The sizes of these nanoparticles in monolayer film are 451 nm.

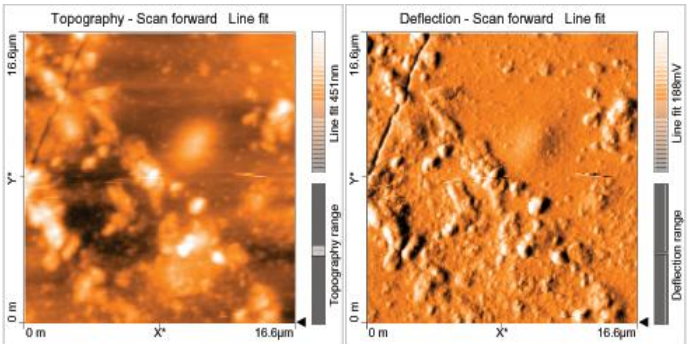

Figure 7. The AFM images of Oleylamine modified Copper nanoparticles.

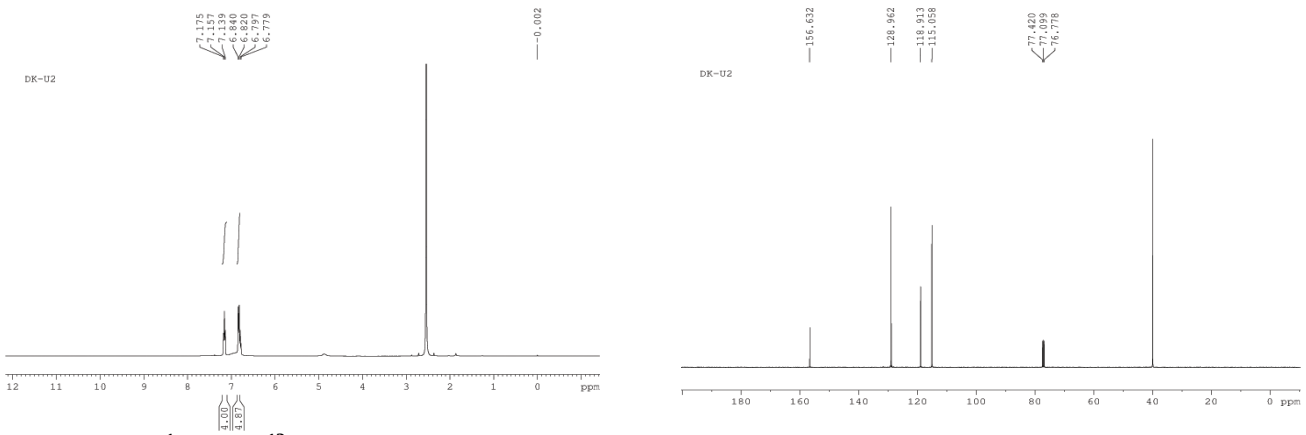

Figure 8 (a , b). ^{1}H and ^{13}C NMR Spectra for Diphenyl ether Copper Nano-U2

Conclusions

In conclusion, a novel, easy, and economical method for the synthesis of diphenyl ethers has been developed using Copper nanoparticles as a catalyst. The process is simple and allows the formation of a diverse range of diphenyl ethers in excellent yields. Overall, this methodology offers competitive advantages such as recyclability of the catalyst without further purification or without using additives or cofactors, low catalyst loading, broad substrate applicability, and high yields in short reaction times.

Acknowledgment

Authors are grateful to the Principal, Muthurangam Govt Arts College, and Vellore for providing facilities to undertake this work.

References

1. Petkov. V., Wanjala B. N., Loukrakpam. R., Luo. J., Yang. L., Zhong. C.J., Shastri. S., (2012) Nano Letts, 12, 4289-4299.
2. Yin. B., Fang. J., Luo. B., Wanjala. R. D., Ng. M. S., Li. Z., Hong. J., Whittingham, C.J. Zhong. M. S. (2012) Nanotechnology, 23, 305404-305410.
3. Veronica Sáez and Timothy J. Mason. (2009) Molecules, 14 4284-4299.
4. Yang. L., Shan. S., Loukrakpam. R., Petkov. V., Ren. Y., Wanjala. B., Engelhard. M., Luo. J., Yin. J., Chen. Y., Zhong. C.J.. (2012) J. Am. Chem. Soc, 134, 15048-15060.
5. Petkov.V., Yang. L., Yin. J., Loukrakpam R., Shan. S., Wanjala. B., Luo. J., Chapman. K. W., Zhong. C. J.. (2012) Phys. Rev. Lett, 109, 125504-125509.
6. Mukundan. V., Wanjala. B. N., Loukrakpam. R, Luo. J, Yin. J, Zhong. C J, Malis. O. (2012) Nano technology, 23, 335705-335710.
7. Khanna. P.K., Gaikwad. S., Adhyapak. P.V., Singh. N. and Marimuthu. R.. (2007) Materials Letters, 61, 4711–4714
8. Rica Boscencu, Mihaela Ili, Radu Socoteanu, Anabela Sousa Oliveira, Carolina Constantin, Monica Neagu, Gina Manda and Luis Filipe Vieira Ferreira. (2010) Molecules, 15, 3731-3743.
9. Premkumar. T., Kurt E. Geckeler. (2006) Journal of Physics and Chemistry of Solids, 67, 1451–1456.
10. 10. Wang Jisen,Yang Jinkai, Sun Jinquan and Bao Ying. (2004) Materials and Design, 25, 625–629.
11. Wang Jisen, Yang Jinkai, Sun Jinquan, Bao Ying. (2004) Materials and Design, 25, 625–629.
12. Andrea Fornara, Petter Johansson, Karolina Petersson, Stefan Gustafsson, Jian Qin, Eva Olsson, Dag Ilver, Anatol Krozer, Mamoun Muhammed, and Christer Johansson,Tailored Magnetic. (2008) Nano Lett, Vol. 8, No. 10.
13. Suribabu Jammi, Sekarpandi Sakthivel, Laxmidhar Rout, Tathagata Mukherjee, Santu Mandal, and Tharmalingam Punniyamurthy. (2009) J. Org. Chem, 74, 1971–1976.

14. Teng Yuan Dong, Chen Ni Chen, Hsiu Yi Cheng, Chiao Pei Chen and Nai Yuan Jheng. (2011) Inorganica Chimica Acta, 367, 158–165.
15. Arul Dhas. N., Paul Raj. C., and Gedanken. A.. (1998) Chem. Mater, 10, 1446-1452.
16. Dinesh Karthik. A., Geetha. K. (2013) Journal of Applied Pharmaceutical Science, 3, 016- 021.
17. Masoud Salavati Niasari, Fatemeh Davar and Noshin Mir. (2008) Polyhedron, 27, 3514–3518.
18. Wen Yin K,Wei Hung Chen ,Ching Yuan,Cheng Kaun Jiuh and Lin. (2009) Nanoscale Res Lett, 4,1481–1485.
19. Masoud Salavati Niasari,Noshin Mir and Fatemeh Davar. (2010) Applied Surface Science, 256, 4003 – 4008.
20. Dinesh karthik. A. and Geetha. K . (2014) Int.J.Nano Dimens. 5(4): 321-327, Autumn 2014 ISSN: 2008-8868.
21. Dinesh karthik. A. and Geetha. K . (2013) National Confererence on Nanometerials (NCONM' 13). 236-240.
22. Sundaram Ganesh Babu and Ramasamy Karvembu. (2011) Industrial & Engineering Chemistry Research, 50, 9594–9600.
23. Shama Rehman, Mumtaz. A. and Hasanain. S. K. (2011) J Nanopart Res, 13, 2497–2507.
24. Wanjala. B ., Fang. B., Shan. S., Petkov. V., Zhu. P., Loukrakpam. R. (2012), Chem. Mater, (ASAP).
25. Xiaojun Zhang, Dongen Zhang, Xiaomin Ni and Huagui Zheng. (2008) Solid State Electronics, 52, 245–248.
26. Dinesh karthik. A. and Geetha. K . (2013) Jai *tech Publications, Chennai*, 236-240. ISBN: 978-93-80624-75-4.
27. Jolivet. J. P, Barron. A. R., Wiesner. M. R, Bottero. J.Y. (2007) Nanoparticle fabrication., Eds, McGraw-Hill New York,
28. Cullity. B.D., (1978) "Elements of X-ray Diffraction", Addison Wesley Pub.Co.
29. Narayanan. R., El-Sayed. M.A.. (2004) J. Am. Chem. Soc, 126 7194–7195.

*****